

INDUSTRIAL

# CERAMICS

SPECIAL ISSUE TECNARGILLA '08

WWW.FDSETTMAR.COM

**Stampi e Attrezzature per Ceramiche**



**FDS  
ETTMAR**  
S.p.A.

F.D.S. ETTMAR S.p.A.  
41049 SASSUOLO (MO) ITALY  
VIA DELL'ARTIGIANATO 12  
TEL. +39 0536 997611  
FAX +39 0536 997666  
e-mail: Info@fdsettmar.Com

Prodotto e certificato con Autocollante CE  
per il settore ceramico  
Modello 125, 130, 135, 140, 145, 150, 155, 160, 165, 170, 175, 180, 185, 190, 195, 200, 205, 210, 215, 220, 225, 230, 235, 240, 245, 250, 255, 260, 265, 270, 275, 280, 285, 290, 295, 300, 305, 310, 315, 320, 325, 330, 335, 340, 345, 350, 355, 360, 365, 370, 375, 380, 385, 390, 395, 400, 405, 410, 415, 420, 425, 430, 435, 440, 445, 450, 455, 460, 465, 470, 475, 480, 485, 490, 495, 500, 505, 510, 515, 520, 525, 530, 535, 540, 545, 550, 555, 560, 565, 570, 575, 580, 585, 590, 595, 600, 605, 610, 615, 620, 625, 630, 635, 640, 645, 650, 655, 660, 665, 670, 675, 680, 685, 690, 695, 700, 705, 710, 715, 720, 725, 730, 735, 740, 745, 750, 755, 760, 765, 770, 775, 780, 785, 790, 795, 800, 805, 810, 815, 820, 825, 830, 835, 840, 845, 850, 855, 860, 865, 870, 875, 880, 885, 890, 895, 900, 905, 910, 915, 920, 925, 930, 935, 940, 945, 950, 955, 960, 965, 970, 975, 980, 985, 990, 995, 1000

2008

M.A. SERRY

Assessment of the Egyptian clay deposits for ceramic industries: a review paper

111

K. DANA, S.K. DAS

Enhanced resistance to thermal cycling of slag-containing vitrified porcelain tiles

121

M.H. AMIN, A. KAZEMZADEH, MOHSEN AMIN-EBRAHIMABADI, N. SAHA-CHAUDHURY, V. SAHAIWALLA

Interactions of magnesia castables used in steelmaking with calcium aluminate slag

125

F. VERNILLI, S.N. SILVA, A.F. SIQUEIRA, E.F. LEITE, E. SAITO, V.F. NASCIMENTO, E. LONGO

Probabilistic neural network to predict cracks in taphole mud used in blast furnaces

133

R. SARKAR, M.K. DAS, S.K. DAS

Development of an acid resistant porous pot using rice husk ash waste

139

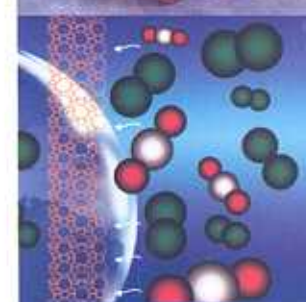
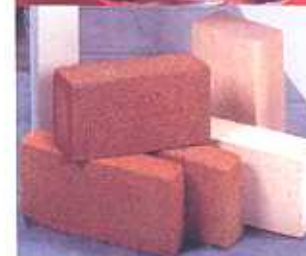
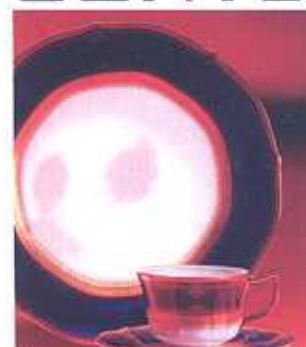
J. VLEUGELS

Fabrication, wear and performance of ceramic cutting tools

145



# CONTENTS





**Mohamad Hassan Amin**

He got Ph.D. Degree in Material Engineering (Ceramics) from the Material and Energy Research Centre (Ministry of Science, Research and Technology, Tehran) in 1999. He was employed by the Shimipejoubeshvar Company as a director of production for magnesia and alumina refractories products from 1989 to 1992. He also worked as vice chancellor (head of research) in Azad University of Yazd for 2 years. He then joined the faculty of Materials and Energy Research Center (MERC) in 1999. He is now in the MERC as an assistant professor in the Ceramic Department.

M.H. Amin<sup>1</sup>, A. Kazemzadeh<sup>1</sup>, Mohsen Amin-Ebrahimabadi<sup>2</sup>,  
N. Saha-Chaudhury<sup>2</sup>, V. Sahajwalla<sup>2</sup>

## Interactions of magnesia castables used in steelmaking with calcium aluminate slag

*Slag penetration into a magnesia refractory castable was investigated by the crucible test method. A synthetic calcium aluminate slag system has been used to corrode a commercial magnesia mix refractory for 1, 2, 3, 4, 5 and 6 h at 1450 °C and 1600 °C. It has been shown that the penetration rate was controlled by a diffusion mechanism at 1450 °C, capillaries being the main channels of initial slag penetration into the refractory. In the penetration process, calcium silicate was formed on the surfaces of MgO grains, and around them by reaction between the grain boundary and mayenite, as a main phase of slag with a low melting point. Dissolution of the refractory components in the slag supported the penetration process at 1600 °C. In this case, dissolution of the refractory components in the slag not only makes new open channels, but also changes the local slag composition, resulting in a decrease of viscosity and an increase of surface tension of the slag.*

### 1. Introduction

In recent years demand for clean metals has increased rapidly. The growing demand for high metals purity and cleanliness requires better control, and therefore a better understanding, of the interactions of refractory with slag and the metal phase in steelmaking. Refractories, as linings of ladles and tundishes, cannot avoid contact with molten steel and slags. The interaction of refractories with their surroundings in high temperature industries remains one of the major challenges. The materials must not only tolerate high temperature but also withstand mechanical stresses, as well as resist attack by liquids such as molten metal and slags.

<sup>1</sup>Material and Energy Research Center, Tehran, Iran; <sup>2</sup>School of Materials Science and Engineering, UNSW, Sydney, Australia.

The most significant trend in refractories technology in the last two decades has been the ever increasing use of monolithic (or unshaped) refractories such as castables which now, in many countries, account for more than 50% of total production due to their quicker and cheaper installation, and properties approaching those of shaped (brick) refractories. Magnesia castables are unshaped refractories commonly used in steelmaking for the maintenance of tundishes. Therefore, a fundamental understanding of the dissolution behaviour of magnesia castables into molten slag is important in steelmaking.

Many researchers have conducted experimental investigations of penetration and corrosion of magnesia castables by slags. These studies showed that the rate of slag penetration increases with increasing pore radius,<sup>1</sup>  $Al_2O_3$  and Fe concentration in the slag,<sup>1,4</sup> test temperature,<sup>1</sup> and with decreasing slag basicity (C/S ratio)<sup>1,4,5,6</sup> as a result of the high capability of dissolving magnesia in the slag.<sup>1-5</sup> Molnar *et al* have studied the interaction of molten silicate and ferritic-calcium slags with magnesite refractories. They suggest that slags of the system  $FeO-Fe_2O_3-CaO$  penetrate more readily beneath the surface of the refractories than the silicate slags, but show lower chemical aggressivity.<sup>7</sup> The effect of the slag type on penetration and corrosion resistance of high purity sintered and fused magnesia has been reported by Zhang *et al*.<sup>8</sup> Some researchers have shown that reaction between CaO in the slag and  $Al_2O_3$  in the castable makes low-melting calcium aluminates, while reaction between CaO in slag and  $Al_2O_3$  in brick results in the formation of spinel at the slag/grain interface.<sup>9</sup> As a result, MgO bricks have higher slag resistance than MgO castables.<sup>8</sup> The penetration and corrosion mechanisms of magnesia castables by silicate slags was investigated.<sup>4</sup> Firstly, the slag, as a single liquid phase, penetrated the castable via the open pores; secondly, the penetrating slag reacted with the surrounding MgO; and finally, the ions (e.g. Ca and Fe) from the slag penetrated more deeply via a diffusion processes.<sup>4</sup> Yu *et al* suggested that the penetration rate of slag into the refractory is related to the corrosion rate.<sup>10</sup> Studies reported in the literature have shown that interactions between slag and refractory materials are dependent on both the slag composition and the type of refractory material.

The corrosion of a refractory is a very complex phenomenon involving not only chemical wear (corrosion) but also physical/mechanical wear (such as erosion/abrasion) processes, which may act synergistically. Corrosion of the lining material in contact with slag is usually described on the basis of the following phenomena: dissolution, which is a chemical process by which the refractory materials are continuously dissolved; and penetration, by which the slag penetrates into the refractory and causes erosion, which is the abrasion process of the refractory material exposed to slag movement.

There exist many reports on the corrosion of magnesia refractories by various slags<sup>2,6,9,11,12</sup> and studies have been done to investigate metal/MgO refractory

interactions in steelmaking.<sup>13-19</sup> Despite these studies, the penetration and corrosion mechanism of commercial magnesia castables by calcium aluminate slags have not yet been studied. In the present work, a synthetic calcium aluminate-slag system has been used to corrode a commercial magnesia mix refractory for various temperatures and times. The investigation is worthwhile, because corrosion of these materials usually occurs in contact with synthetic slag that carried over from the ladle, and there are still some obscure points concerning the relevant parameters which may influence this problem that generally dominates the refractory life.

## 2. Experimental details

The corrosion of commercial magnesia refractory by calcium aluminate slag was studied using a static crucible corrosion test, with a fixed amount (50g) of powder slag placed in each crucible. Table 1 shows the chemical composition of the magnesia mix. The slag mixtures of fixed composition were prepared by weighing 173.16g reagent grade calcium carbonate ( $CaCO_3$ ) and 157.57g aluminum hydroxide ( $Al(OH)_3$ ), wet-mixing them with ethanol in an alumina ball mill for 3 h and drying at 120 °C for 24 h.

The test crucibles were prepared by drilling a hole 10 cm diameter x 7 cm deep cup cut out of high alumina brick and then lining them (to 20mm thickness) with the magnesia castable powder mixed with 10 wt% of water, by patching. In this case, there is a condition the same as the situation of a magnesia castable powder mixed lining on high alumina brick working layer of tundishes, which are used in the Mobarakeh Steel Plant. A schematic figure of the crucible is shown in Fig. 1. The slag was melted in a Pt crucible at 1650 °C for 3 h and castable crucibles were heated at 1200 °C for the

Table 1. Chemical composition of castable

Oxide	MgO	CaO	SiO <sub>2</sub>	Fe <sub>2</sub> O <sub>3</sub>	Al <sub>2</sub> O <sub>3</sub>	K <sub>2</sub> O	Na <sub>2</sub> O
Mass%	95.32	1.53	2.43	0.11	0.08	0.10	0.43

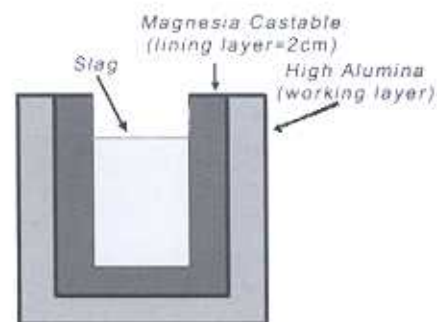


Figure 1. Schematic figure of crucible

same time. The slag was then cast into the magnesia crucible inside the furnace immediately. The slag penetration was carried out in the furnace in air atmosphere at 1450 °C and 1600 °C for 1, 2, 3, 4, 5 and 6 h. After holding each crucible for a specified fixed time, it was taken out of the furnace and cooled by blowing cold air from just above the crucible for 1h. To study the microstructure and phases present in the castable without slag present, one sample was fired following the same heating program used for the corrosion test.

The slag penetration was determined on a cut face of the crucible mounted in epoxy resin. Chemical analyses were performed using X-ray fluorescence spectrometer (ARL XRF). An X-ray diffraction technique was used to identify phase changes using a Philips-112 X-ray diffractometer, in the angle range 5 to 80° with a step size of 0.02°. The cross-section of the used lining was examined by optical microscopy (Zeiss Oxi-Vert 200) and the observation of microstructure was performed on polished faces using a scanning electron microscope (SEM) equipped with X-ray spectroscopy (LEO 460). The apparent porosity and density were determined according to ASTM C20-87. The pore size distribution was determined by a mercury porosimeter according to DIN EN 993.

### 3. Experimental results

#### 3.1. Characterization of refractory and slag

The apparent porosity, bulk density and the average pore radius of the samples after drying were 8.4%, 2.96g/cm<sup>3</sup> and 0.15 μm, respectively.

XRD patterns of magnesia castable and synthesized slag are shown in Figs. 2 and 3 respectively. The main phase of the castable sample is MgO periclase. In addition to the MgO main peak, weak peaks also exist in the XRD pattern which are attributed to monticellite (CaO.MgO.SiO<sub>2</sub>). The  $\frac{CaO}{SiO_2}$  ratio of the used magnesia castable was less than 1. According to references, monticellite (CMS), forsterite (2MgO.SiO<sub>2</sub>) and magnesioferrite (MgO.Fe<sub>2</sub>O<sub>3</sub>) would be expected in addition to periclase under these conditions.<sup>20-22</sup> However, X-ray diffraction indicates only the presence of monticellite while forsterite and magnesioferrite can not be identified.

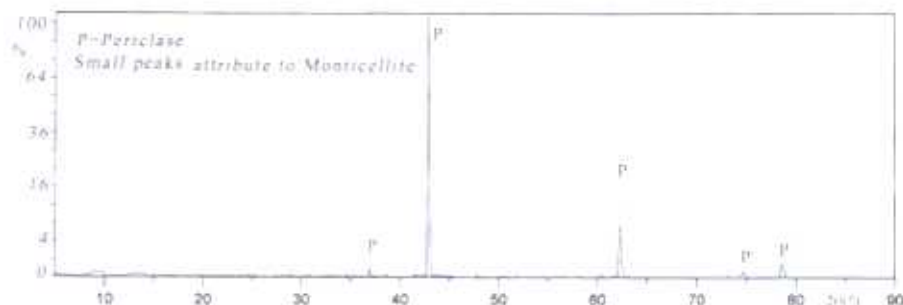


Figure 2. Partial XRD pattern of magnesia castable

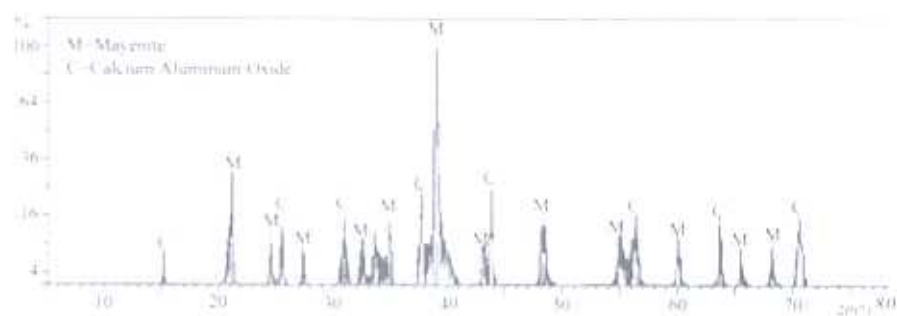


Figure 3. Partial XRD pattern of synthesized slag

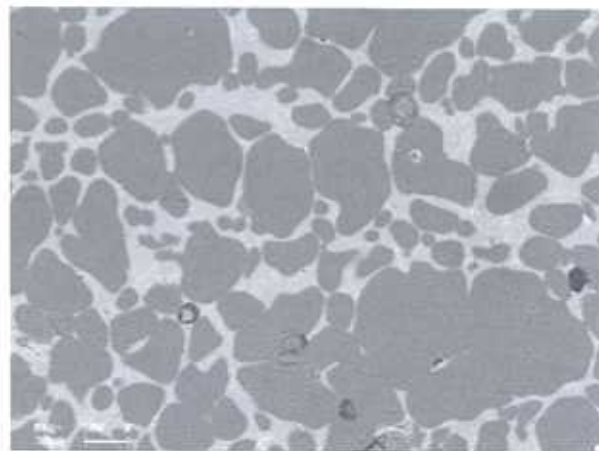


Figure 4. SEM micrograph of the fired magnesia castable microstructure before penetration

Mayenite is the main phase of the slag sample in Fig. 3, which matches with the XRD pattern in PDF 9-0413 reference card with chemical formula of Ca<sub>12</sub>Al<sub>14</sub>O<sub>33</sub>. In addition to the main phase, other weak peaks are also observed which are attributed to calcium aluminium oxide (3CaO.Al<sub>2</sub>O<sub>3</sub>) with melting point 1900 °C, which matches with the XRD patterns in PDF 8-0005 and 6-0495 reference cards.

#### 3.2. Microstructure and phases

A backscattered electron image of the fired magnesia castable microstructure before penetration is shown in Fig. 4. It was observed that a grain boundary phase

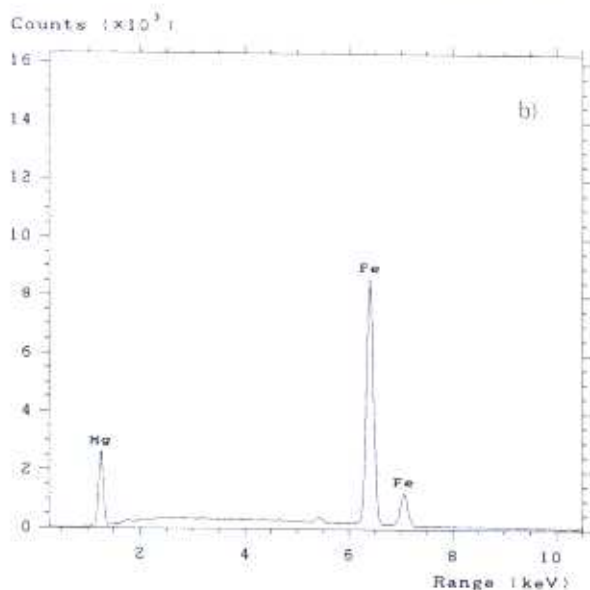
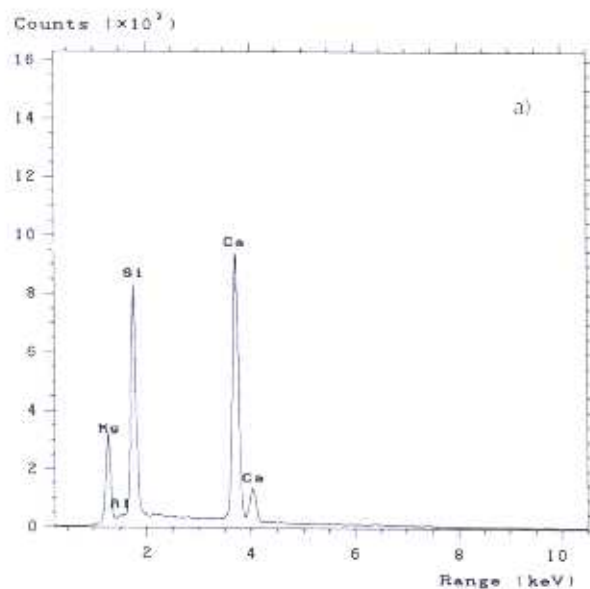


Figure 5. X-ray spectroscopy of (a) the main grain boundary phase and (b) bright phase in the fired magnesia castable microstructure before penetration

Table 2. Elemental analysis of secondary phases in the fired magnesia castable

Element	Mg	Ca	Si
Mol%	15.47	13.16	14.24

wetted the MgO grains. Fig. 5(a) shows the typical elemental analysis pattern of the secondary phase among the periclase particles, and the mean of the results is shown in Table 2. It is shown by X-ray diffraction as well that the main grain boundary phase is based on monticellite. Monticellite is the most undesirable phase because of its low melting point (1488 °C) which decreases the refractoriness of the product<sup>22, 23</sup>. The data in Table 2 confirm that these phases have similar

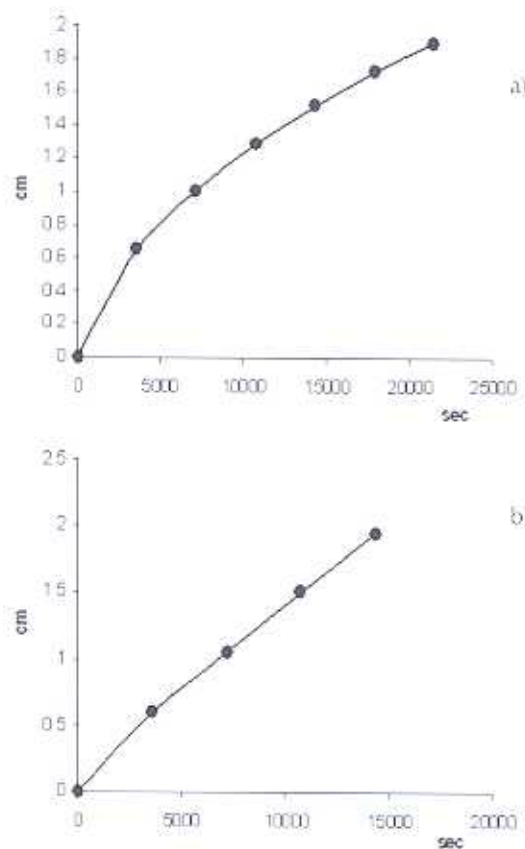


Figure 6. Relation between penetration time (sec) and thickness of penetrated slag (cm) in the castable crucible at (a) 1450 °C and (b) 1600 °C

stoichiometric compositions of monticellite accompanying forsterite. This could be due to dissolution of some forsterite in monticellite and vice versa<sup>24</sup>. Apart from MgO and monticellite, there is a bright phase present in the microstructure. Fig. 5(b) shows the typical elemental analysis pattern of this phase. According to references,<sup>21</sup> this phase could be magnesiumferrite (melting point, 1750 °C) with higher atomic number to appear as a lump pocket due to low solubility of this phase in monticellite.

### 3.3. Slag penetration into castable

The relationships between penetration time and thickness of penetrated slag in the castable crucible at different temperatures are shown in Fig. 6. The curve for the temperature of 1450 °C was a parabolic curve; whereas the curve representing data at the temperature of 1600 °C was linear (the correlation coefficient is equal to 1). A plot of thickness of penetrated slag in the castable crucible,  $h$ , against  $\sqrt{t}$  for samples at 1450 °C (shown in Fig. 7) indicates a good linear relationship, thus confirming the parabolic behaviour. The corrosion rate at 1600 °C was faster than at the lower temperature, since at this temperature, slag penetrates throughout the whole magnesia castable lining just after 4 hour and reaches the high alumina brick working layer.

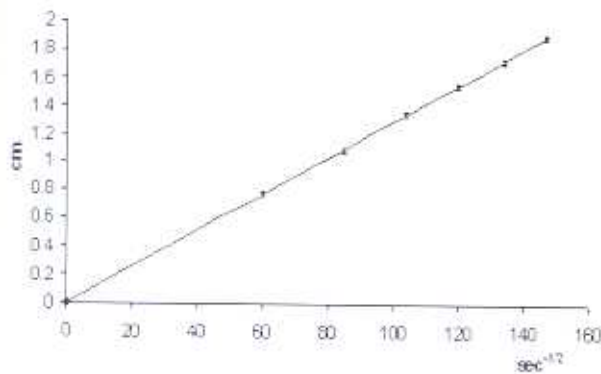


Figure 7. Relation between thickness of penetrated slag ( $h$ ) and  $\sqrt{t}$  time at 1450 °C

## 4. Discussion

### 4.1. Penetration rate of slag

Two distinct slopes indicate that the penetration of magnesia castable with calcium aluminate slag could be dictated by different mechanisms at the two temperatures. The parabolic curve is a sign that the penetration rate at 1450 °C is controlled by a diffusion mechanism. In this case the rate equation could be as follows:

$$h^2 = k't \quad \text{or} \quad \dot{h} = k\sqrt{t} \quad (1)$$

where  $h$  is the slag penetration depth (cm),  $t$  is time (sec) and  $k'$  ( $\text{cm}^2/\text{sec}$ ) and  $k$  ( $\text{cm}/\text{sec}^{1/2}$ ) are rate constant of penetration. A plot of  $h$  against  $\sqrt{t}$  time, shown in Fig. 7, indicates a good linear relationship and yields an overall rate constant of  $0.013 \text{ cm}/\text{sec}^{1/2}$ .

Capillaries, such as open pores and microcracks, are the main channels of initial slag penetration into a refractory. In this case, the penetration rate  $dh/dt$  of slag into a capillary can be expressed by Poiseuille's law:<sup>21</sup>

$$\frac{dh}{dt} = \frac{r^2 \Delta P}{8\eta h} \quad (2)$$

where  $r$  is the capillary radius,  $\Delta P$  the capillary sucking pressure and  $\eta$  is viscosity of the slag. The term  $\Delta P$  is expressed by

$$\Delta P = 2\gamma \cos\theta / r \quad (3)$$

where  $\gamma$  is the slag surface tension and  $\theta$  the wetting or contact angle. By eliminating  $\Delta P$  from equation (2):

$$\int_0^h h dh = \frac{r^2 \gamma \cos\theta}{4\eta} \int_0^t dt \quad \text{So:} \quad h^2 = \frac{r^2 \gamma \cos\theta}{2\eta} t \quad (4)$$

Comparison between equations (1) and (4) gives the rate constant of penetration as follows:

$$k = \sqrt{\frac{r^2 \gamma \cos\theta}{2\eta}} \quad (5)$$

### 4.2. Slag viscosity and surface tension

Most models for calculating viscosity are based on numeric adjustments starting from experimental data,

and they are rarely based on the slag structure.<sup>26</sup> The Urbain model estimates the viscosity of slags as a function of chemical composition and mineralogical nature.<sup>26</sup> This model describes temperature dependence of the slag viscosity ( $\eta$ ) using the Weymann equation:<sup>9</sup>

$$\eta (\text{Ns}/\text{m}^2) = 0.1QT \exp\left(\frac{1000P}{T}\right) \quad (6)$$

where  $T$  is the absolute temperature, and  $P$  and  $Q$  are constants obtained by the following equations<sup>9</sup>:

$$Q = \exp(-11.6725 - 0.263P) \quad (7)$$

$$P = P_0 + P_1N + P_2N^2 + P_3N^3 \quad (8)$$

$$P_0 = 13.8 + 39.9355\alpha - 44.049\alpha^2 \quad (9)$$

$$P_1 = 30.481 - 117.1505\alpha + 129.9978\alpha^2 \quad (10)$$

$$P_2 = 40.9429 + 234.0486\alpha - 300.04\alpha^2 \quad (11)$$

$$P_3 = 60.7619 - 153.9276\alpha + 211.1616\alpha^2 \quad (12)$$

$N$  is the mole fraction of  $\text{SiO}_2$  in the slag and  $\alpha$  is the mole fraction of  $\text{CaO} + \text{MgO} / \text{CaO} + \text{MgO} + \text{Al}_2\text{O}_3$  in the slag. In this study,  $\alpha$  is 0.63; therefore slag viscosity can be expressed by following equation:

$$\eta (\text{Ns}/\text{m}^2) = 3.02 \times 10^{-4} T \exp\left(\frac{21451.63}{T}\right) \quad (13)$$

The viscosity values of the original slag at temperatures of 1450 °C and 1600 °C are 1.33 and 0.53  $\text{Ns}/\text{m}^2$  respectively. It was found that the viscosity of the liquid phase decreased with increasing temperature. Thus, the rate constant of penetration increased accordingly. The surface tension,  $\gamma$ , of the slag was calculated by the following equation:<sup>9</sup>

$$\gamma (\text{N}/\text{m}) = (sF_s + s'F_{s'} + c_aF_{c_a} + mF_{m'}) \quad (14)$$

In the above equation,  $s$  is the mole fraction of a cation of an oxide component. The mole fraction of cations in the original slag is 0.00, 0.54, 0.46 and 0.00 for cations of Si, Al, Ca and Mg respectively.  $F$  is the constant known as the surface tension factor of a cation of an oxide component. This factor is 0.34, 0.34, 0.47 and 0.58 for cations of Si, Al, Ca and Mg respectively.<sup>9</sup> Therefore, the surface tension,  $\gamma$ , of the original slag was calculated as 0.3998  $\text{N}/\text{m}$ .

### 4.3. Slag penetration phenomenon and associated mechanism

The average pore radius was about  $1.5 \times 10^{-7} \text{ m}$  and the viscosity of the original slag at a temperature of 1450 °C is 1.33  $\text{Ns}/\text{m}^2$  or 13.3 Poise, also assuming  $\theta \ll 90^\circ$  for basic slags, thus  $\cos\theta = 1$ ,<sup>27</sup> and the rate constant gives:

$$k = \sqrt{\frac{0.3998 \text{ Nm}^{-1} \times 1.5 \times 10^{-7} \text{ m}}{2 \times 1.33 \text{ N} \cdot \text{Sec} \cdot \text{m}^{-2}}} = 1.50 \times 10^{-4} \text{ m} \cdot \text{sec}^{-1/2} = 0.015 \text{ cm} \cdot \text{sec}^{-1/2} \quad (15)$$

There is a small difference between the calculated rate

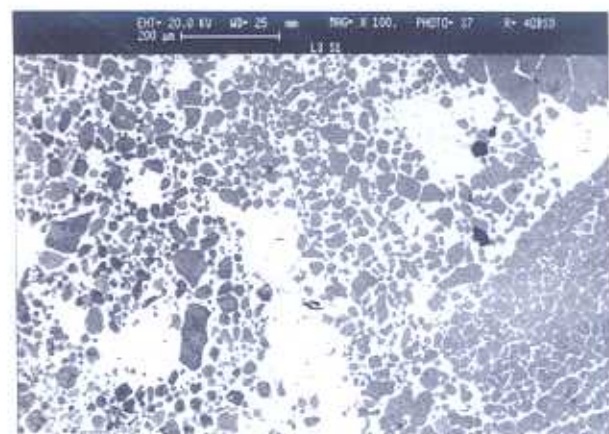
constant and experimental rate constant. The infiltration rate is affected by the temperature gradient in the refractory. When the temperature decreases, the viscosity increases, so in fact, the experimental rate constant decreases.

Slag temperature has a large effect on the penetration depth through its effect on  $\eta$ . Clearly, what is missing from equation (5) is a factor describing the microstructure of a refractory, although this can be incorporated in the  $r$  term. Fig. 8 shows the backscattered electron image of the refractory matrix in the crucible, after slag reaction at 1450 °C for 6 hour, along with the typical elemental analysis pattern of the secondary phase among the periclase particles. It is evident that the main bright colour phase is based on calcium aluminate. It was observed that the MgO grain boundaries were corroded by slag penetration. The image in Fig. 8 also shows the degree to which MgO grains were isolated in the slag. It was confirmed by XRD analysis that the corroded sample had calcium aluminate phases co-existing with periclase. Fig. 9 shows the XRD pattern of the sample taken from the slag-penetrated portion of the castable crucible, after slag reaction at 1450 °C for 6 hour. The diffraction pattern showed the presence of periclase, mayenite and dicalcium silicate (PDF 3-0753).

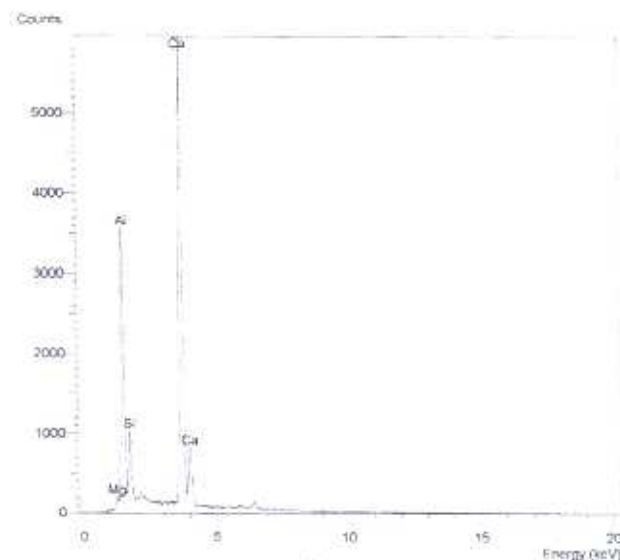
From equation (5) it can be seen that at higher temperature the penetration rate increases with decreasing slag viscosity. It is this relation which means that on first contacting the hot surface liquid, slag penetrates by capillary or wetting suction to depth  $h$  down open pores of radius  $r$ , dependent in large part on the temperature of the refractory. As temperature decreases away from the hot phase, slag viscosity increases so the slag is too viscous to penetrate further.

As shown in Fig. 6 (b), a plot of the thickness of penetrated slag in the castable crucible ( $h$ ) against time (second) at a temperature of 1600 °C was linear (because the correlation coefficient is equal to 0.998)<sup>26</sup>. Examination of slag in the corroded sample at 1600 °C by XRD has shown the dissolution of the refractory components in the slag. As apparent from Fig. 10, the XRD patterns of slag in the surface of the refractory after a corrosion test at 1600 °C show the existence of both periclase (MgO) and spinel  $MgAl_2O_4$  (PDF 5-0672) accompanying calcium aluminate slag. In addition, the diffraction pattern also showed the weak peaks that indicate gehlenite compound ( $2CaO \cdot Al_2O_3 \cdot SiO_2$ , refer to PDF card 35-0755). The existence of silicate phase in slag indicates that corrosion of the MgO castable by calcium aluminate slag was related to the dissolution of both MgO and monticellite ( $CaO \cdot MgO \cdot SiO_2$ ). In this case, the mechanism is as follows. MgO in the castable reacted with  $Al_2O_3$  to form spinel and CMS in the

castable (mainly in the matrix) reacted with calcium aluminate from the slag diffused to the castable, to form  $2CaO \cdot Al_2O_3 \cdot SiO_2$  (melting point, 1593 °C)<sup>29</sup>, and thus dissolved in the slag. The melting point of monticellite is 1488 °C, so it should be solid phase at 1450 °C but a liquid phase at 1600 °C which would dissolve quickly in the local slag. As a result, it can be



a)



b)

Figure 8. (a) SEM micrograph of slag-penetrated portion of the castable crucible, after slag reaction at 1450 °C for 6 hour, and (b) X-ray spectroscopy of the bright phase

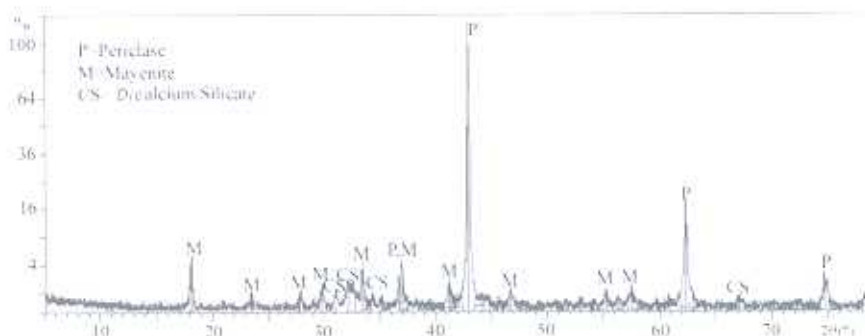


Figure 9. Partial XRD pattern of corroded samples



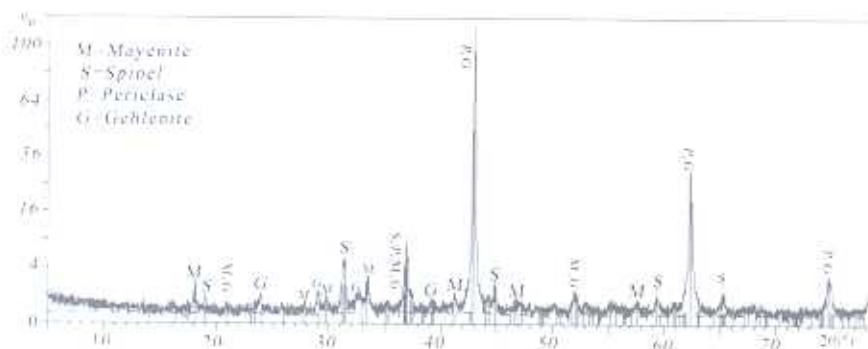


Figure 10. XRD patterns of slag in the surface of refractory after corrosion test at 1600 °C

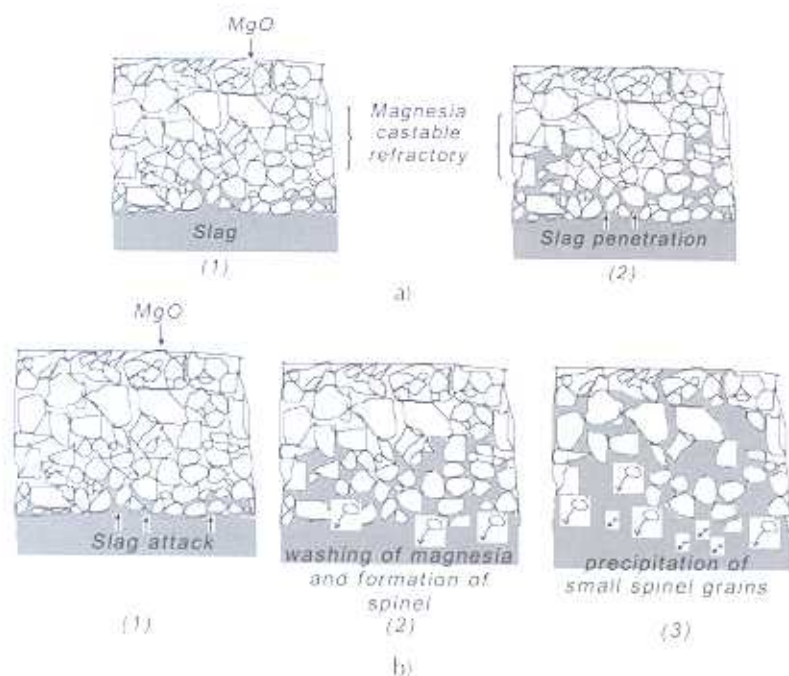


Figure 11. Corrosion mechanism of magnesia refractory (a) at 1450 °C and (b) at 1600 °C

concluded that with increase of temperature, dissolution of refractory into slag leads to a deviation of the mechanism from diffusion.

Dissolution at refractory / slag interfaces is governed by (a) chemical reaction (or solution) at the interface, or (b) transport (or diffusion) of reacting species through the liquid boundary layer. Direct dissolution can be reaction or interface controlled when the diffusivity of reaction products is faster than the rate of chemical reaction at the interface. In this case the dissolution process may be directly controlled by a reaction that is of first order with respect to a reactant species. Dissolution of the refractory components, making new open channels (e.g., by connecting some closed pores) leads to further penetration. In this case, the slag as a liquid phase, is driven into the refractory by the capillaries.<sup>19</sup>

Dissolution of the refractory components in the slag not only makes new open channels, but also changes the local slag composition, and therefore, the slag

viscosity and surface tension. The application of the Urbain model to estimate viscosity confirms that when the slag basicity increases, as dissolution of the MgO in slag occurs, viscosity decreases because MgO acts as a modifier.<sup>20</sup> In addition, according to equations (6-12), the concentration of  $Al_2O_3$  in the liquid phase decreased by assuming that spinel was precipitated from the liquid

phase (as shown in Fig. 10) leading to an increase in the constant  $P$ . Also, the surface tension of the liquid phase increased due to a decrease in the percentage of  $Al_2O_3$  having a small surface tension factor due to the precipitation of spinel, and an increase in the percentage of MgO having a large surface tension factor due to dissolution of MgO in the liquid phase. If the slag viscosity decreases or surface tension increases, then according to equation (5), it will accelerate the penetration. From the above discussion, it is concluded that the slag penetration behaviour changed with increase in temperature; the slag composition was changed by dissolution of MgO grains in the slag, resulting in a decrease of viscosity and an increase in surface tension. The overall mechanism is schematically represented in Fig. 11.

## 5. Conclusions

Slag penetration studies at 1450 °C and 1600 °C were carried out using the crucible method in order to understand the mechanism of reaction between slag and the refractory, and the influence of reaction temperature on slag penetration into magnesia refractories. The following conclusions have been shown:

- (1) Penetration of magnesia castable refractory by calcium aluminate slag at 1450 °C in a static test indicates the corrosion rate to be controlled by a diffusion mechanism. In this case, capillaries, such as open pores and microcracks, are the main channels of initial slag penetration into the refractory. In the penetration process of the slag, calcium silicate was formed on the surfaces of MgO grains; and around them by reaction between grain boundary and mayenite, as a main phase of slag with a low melting point.
- (2) As the test temperature increased, the corrosion mechanism of the refractory by the slag changed, and

the penetration rate at 1600 °C was faster than at lower temperature. In this case, dissolution of the refractory components in the slag supported the penetration process. Consequently, dissolution of the refractory components in the slag not only makes new open channels, but also changes the local slag composition, resulting in a decrease of viscosity and an increase of surface tension of the slag. Accordingly, they lead to an increase in the penetration rate.

### Acknowledgments

The authors wish to acknowledge the Mobarakeh Steel Plant (Isfahan, Iran) for the financial support of this project.

### References

1. K. Mukai, Z. Tao, K. Goto, Z. Li, T. Takashima, *Refractories (Tokyo)*, 53 (2001), 390-398.
2. P. Zhang, S. Seetharaman, *J. Am. Ceram. Soc.*, 77 (1994), 970-976.
3. Z. Tao, K. Mukai, H. Yonezawa, Y. Yoshimura, *J. Tech. Assoc. Refract. Japan*, 20 (2000), 10-17.
4. S. Zhang, W.E. Lee, N. Li, Proc. of Conf. 'UNITECR '01', Unified Int. Tech. Conf. on Refractories, 7th Biennial Worldwide Congress, Vol. 1, Cancun 4-7, (2001), 65-79.
5. K. Matsui, F. Kawano, K. Nibu, *Refractories (Tokyo)*, 43 (1991), 42-450.
6. S. Zhang, H. Sarpoolaky, N.J. Marriott, W.E. Lee, *British Ceramic Transactions*, 99 (2000), 248-255.
7. L. Molnar, P. Vadasz, M. Kozlovsky, *Ceramics-Silikaty*, 37 (1993), 121-125.
8. J.-H. Woo, D.-H. Kim, S.-M. Kim, *Journal of the Korean Institute of Metals and Materials (South Korea)*, 39 (2001), 835-843.
9. T. Matsui, K. Hiragushi, T. Ikemoto, K. Sawano, *J. Tech. Assoc. Refract. Japan*, 22 (2002), 302-309.
10. Z. Yu, K. Mukai, K. Kawasaki, I. Furusato, *Journal of the Ceramic Society of Japan*, 101 (1993), 533-539.
11. H. Fukuyama, J.R. Donald, J.M. Töguri, *J. Am. Ceram. Soc.*, 80 (1997), 2229-2236.
12. T. Matsui, K. Hiragushi, T. Ikemoto, K. Sawano, *Journal of the Technical Association of Refractories, Japan*, 23 (2003), 11-14.
13. L. Zhao, V. Sahajwalla, *ISIJ International*, 43 (2003), 1-6.
14. V. Sahajwalla, C. Wu, R. Khanna, N.S. Chaudhury, J. Spink, *ISIJ International*, 43 (2003), 1309-1315.
15. M.H. Amin, B. Arfaei, A. Kazemzadah, Proc. of the 9<sup>th</sup> International Chemistry Conference in Africa, University of Dar Es Salaam, (2005) 14-SL18.
16. M.H. Amin, Z. Nemat, B. Akbari, Proc. of the 5<sup>th</sup> Iranian Ceramic Congress, Iran University of Science and Technology, (2004) 11-16.
17. M.H. Amin, B. Arfaei, Proc. of the 5<sup>th</sup> European Continuous Casting Conference, 2005, Nice, France.
18. M.H. Amin, B. Arfaei, Proc. of Iranian Steel Symposium83, Iran Alloy Steel Co., (2005)978-987.
19. M.H. Amin, N. Akbari, Proc. of Iranian Steel Symposium83, Iran Alloy Steel Co., (2005)988-999.
20. M.H. Amin, F. Golestanifard, F. Moztarzadah, *Industrial Ceramics*, 22 (2002), 19-25.
21. T. Taschler, Proc. of Tehran International Conference on Refractories, 4-6 May 2004, 302-320.
22. M.H. Amin, *Industrial Ceramics*, 25 (2005), 27-29.
23. M.H. Amin, F. Moztarzadah, *Journal of Faculty of Engineering (University of Tabriz)*, 29 (2004), 1-10.
24. M.H. Amin, F.A. Hessari, M. Solati, *Industrial Ceramics*, 23 (2003), 205-209.
25. W.E. Lee, S. Zhang, *International Materials Reviews*, 44 (1999), 77-104.
26. J. Madias, E. Brandaleze, M. Bentancour, R. Topolevsky, S. Camelli, Proc. of Conf. 'UNITECR '01', Unified Int. Tech. Conf. on Refractories, 7th Biennial Worldwide Congress, Vol. 1, Cancun, 4-7, (2001), 475-487.
27. B. Sjödin, *Eldfasta Material, Technical Compendium, MEFOS*, (1971).
28. Z.B. Alfassi, Z. Boger and Y. Ronen, *Statistical Treatment of Analytical Data*, Blackwell publishing, CRC press, (2005).
29. W.S. Resende et al, *Journal of the European Ceramic Society*, 20 (2000), 1419-1427.